Orbital Modifications Using Forced Tether-Length Variations

Manuel Martinez-Sanchez* and Sarah A. Gavit†
Massachusetts Institute of Technology, Cambridge, Massachusetts

It is shown that once-per-orbit modulations of the length of an orbiting tether can be used to modify the eccentricity, energy, and line of apsides orientation of its center of mass while maintaining a constant angular momentum and orbital parameter. Appropriate length variation laws are developed and the effects are quantified and interpreted. Several applications are discussed, including modifications to the orbit of a space station, reduction by 30% of the ΔV to launch a satellite to 12 h orbit, and the relocation of the apogee for observation satellites.

I. Introduction

THE common observation of children "pumping" themselves up at a swing by rhythmically shifting their legs' weight has prompted speculation about the possibility of performing fuelless orbital changes using conformable spacecraft.[1,2] Particularly intriguing are the possibilities opened by the advent of ultralong, thin tethers that can be conveniently reeled in and out from a satellite while carrying another body at its end. Obviously, any such reel-unreel operation will set up Coriolis forces that will induce in-plane libration of the tether. To conserve angular momentum, equal and opposite variations will appear in the center of mass orbital angular momentum. If these can be made to resonate with the orbital motion, it is conceivable that the system could bootstrap itself and either increase or decrease the orbital energy without setting up unbounded librations (and getting wrapped up in the process). A clear limitation of any such scheme is the need to supply mechanical power onboard. Another one is the impossibility of modifying the overall angular momentum in this manner, since operation in a central force field is assumed and no internal angular momentum is allowed to accumulate. The question of whether the center of mass motion can be affected by means of forces internal to the mass-tether system is more subtle; although it is true that the acceleration of the center of mass is due to only the net *external* force, nonrigid changes to the configuration of the system can affect the net external force for a given center of mass location and hence can affect the center of mass motion.

In this paper we show how this can be accomplished using a rewindable tether. The practical application of the concept to several space transportation missions is also discussed. The analysis presented here is restricted to the small oscillation of a "dumbbell" satellite whose cable length is assumed fully controllable by means of powered winches on board one or both of the connected masses.

II. Formulation

Forces on an Orbiting Dumbbell

For an extended body, the gravitational net force due to an attracting center includes the familiar radial force due to the total mass at the mass center, plus additional radial and azimuthal force components which are small by comparison (of the order of $(D/r_G)^2$, where D is a typical object length and r_G is the radius vector of the center of mass). These forces are[3]

$$\delta F_r = +\frac{3\mu}{r_G^4}\left(I_r - \frac{1}{2}I_\theta\right) + \text{higher order} \tag{1}$$

$$\delta F_\theta = +\frac{3\mu}{r_G^4} I_{r\theta} + \text{higher order} \tag{2}$$

where μ is the gravitational constant for the attracting center, I_r and I_θ are the body moments of inertia about the radial and azimuthal axes through the body center of mass directions, and $I_{r\theta}$ is the corresponding product of inertia. For a simple two-mass system such as that of Fig. 1, these forces reduce (to second order in ℓ/r_G) to

$$\delta F_r = -\frac{3\mu m_{12}}{r_G^2}\left(\frac{\ell}{r_G}\right)^2\left(1 - \frac{3}{2}\sin^2\alpha\right) \tag{3}$$

$$\delta F_\theta = \frac{3\mu}{r_G^2} m_{12}\left(\frac{\ell}{r_G}\right)^2 \sin\alpha\cos\alpha \tag{4}$$

where m_{12} is the reduced mass, $m_1 m_2/(m_1+m_2)$.

The tension T on the cable joining the two masses depends also upon the motion of the system. A straightforward calculation yields

$$T = +\frac{\mu}{r_G^3} m_{12}\ell(2 - 3\sin^2\alpha) + m_{12}\ell(\dot\alpha + \dot\theta)^2 - \frac{3\mu}{r_G^4} m_{12}\frac{m_1 - m_2}{m_1 + m_2}\ell^2\cos\alpha\left(1 - \frac{5}{2}\sin^2\alpha\right) - m_{12}\ddot\ell \tag{5}$$

where a dot signifies a time differentiation. For a circular orbit and zero libration angle α, Eq. (5) reduces to the more familiar expression $T = 3\mu m_{12}\ell/r_G^3$.

Equations of Motion

With the external forces known, the radial and azimuthal equations of motion for the center of mass of the orbiting dumbbell are (using $m = m_1 + m_2$)

$$m(\ddot r_G - r_G\dot\theta^2) = -\frac{\mu m}{r_G^2} - \frac{3\mu m_{12}}{r_G^2}\left(\frac{\ell}{r_G}\right)^2\left(1 - \frac{3}{2}\sin^2\alpha\right) \tag{6}$$

$$m\frac{\mathrm{d}}{\mathrm{d}t}(r_G^2\dot\theta) = \frac{3\mu}{r_G} m_{12}\left(\frac{\ell}{r_G}\right)^2 \sin\alpha\cos\alpha \tag{7}$$

In addition, since all the external forces are assumed to be central, the overall angular momentum about an axis perpendicular to the orbit must remain constant. This angular momentum must include both that due to the total mass m concentrated at G plus that due to libration about G. Since for the dumbbell the moment of inertia about the libration axis is

Received Jan. 28, 1986; revision received Sept. 22, 1986.

*Associate Professor of Aeronautics and Astronautics. Member AIAA.

†Senior Engineer, Systems Analysis; currently at Martin Marietta Aerospace Corporation. Member AIAA.

$m_{12}\ell^2$, we obtain

$$mr_G^2\dot{\theta} + m_{12}\ell^2(\dot{\alpha} + \dot{\theta}) = L \tag{8}$$

Equations (6), (7), and (8) together govern the tether libration α and the orbital motion of the center of mass G. Notice from Eq. (7) that the *orbital* angular momentum is not conserved in the presence of libration; indeed, from Eq. (8), it must have modulations that are equal and opposite to those due to the libration. It is this "spin-orbit" coupling that we are trying to exploit for orbital modifications.

A useful combination of equations governing α directly is obtained from Eqs. (7) and (8):

$$\frac{\mathrm{d}}{\mathrm{d}t}[\ell^2(\dot{\alpha} + \dot{\theta})] = -\frac{3\mu}{r_G}\left(\frac{\ell}{r_G}\right)^2 \sin\alpha\cos\alpha \tag{9}$$

For a fixed length ℓ and a circular orbit, Eq. (9) is the familiar in-plane libration equation, showing small-amplitude oscillations at a frequency $\sqrt{3}$ times orbital frequency. For noncircular orbits and if the length is made variable, other types of solutions occur, which will be explored shortly.

Variation of Orbital Parameters

The forces given by Eqs. (3) and (4) can be regarded as the product of m times small perturbation accelerations a_r, a_θ, and the center-of-mass orbit can be viewed as a continuously deformed Keplerian orbit instantaneously characterized by a semimajor axis a, eccentricity e, and argument of perigee ω. These orbital elements evolve in time according to the classical perturbation equations:[4]

$$\frac{\mathrm{d}h}{\mathrm{d}t} = r_G a_\theta \tag{10}$$

$$\frac{\mathrm{d}a}{\mathrm{d}t} = \frac{2a^2}{h}\left(\ell\,\sin\theta a_r + \frac{p}{r_G}a_\theta\right) \tag{11}$$

$$\frac{\mathrm{d}e}{\mathrm{d}t} = \frac{p}{h}\left\{\sin\theta a_r + \left[\cos\theta + \frac{r_G}{p}(e + \cos\theta)\right]a_\theta\right\} \tag{12}$$

$$\frac{\mathrm{d}\omega}{\mathrm{d}t} = -\frac{1}{eh}[p\,\cos\theta a_r - (p + r_G)\,\sin\theta a_\theta\} \tag{13}$$

Here, $p = a(1 - e^2)$ is the orbital parameter and h, the orbital angular momentum, is just $r_G^2\dot{\theta}$, not the overall angular momentum L of Eq. (8). We wish to impose at this point the constraint that the libration angle α should remain bounded. Although spinning pumping schemes may be practical, we here restrict attention to nonspinning cases. With reference to Eq. (8), if ℓ is varied cyclically about a constant mean value and α is bounded, the angular momentum $m_{12}\ell^2\dot{\alpha}$ must remain bounded as well. The term $m_{12}\ell^2\dot{\theta}$ may, however, have a slow drift if the orbital energy and hence the mean $\dot{\theta}$ is made to evolve in time as a consequence of the tether modulations. Then this drift of $\dot{\theta}$ would be itself of order ℓ^2 and that of $m_{12}\ell^2\dot{\theta}$ would be of order ℓ^4, hence negligible in our analysis. In an alternative to be studied shortly, (ℓ/r_G) will be modulated with constant amplitude, thus letting ℓ drift as the orbit dimension does. In that case, $m_{12}\ell^2(\dot{\alpha} + \dot{\theta}) = m_{12}(\ell/r_G)^2 r_G^2\dot{\theta}(1 + \mathrm{d}\alpha/\mathrm{d}\theta)$ will have the same long-range behavior as $r_G^2\dot{\theta}$. In either case, Eq. (8) shows that *the orbital angular momentum $h = r_G^2\dot{\theta}$ must remain constant in an average sense.*

Using the notation $\langle\ \rangle$ to indicate an average taken over many orbits such that the rapid intraorbital oscillations are eliminated, we then have

$$\left\langle\frac{\mathrm{d}h}{\mathrm{d}t}\right\rangle = 0 \tag{14}$$

In the same average sense, the semimajor axis and the eccentricity must therefore be related through the Keplerian equation

$$h^2 = \mu a(1 - e^2) = \langle\mathrm{const}\rangle \tag{15}$$

and the parameter $p = h^2/\mu$ is also a long-term constant. Thus, only Eqs. (12) and (13) need be retained and solved. This we will do by first solving the libration equation for α (for a prescribed tether variation law), calculating a_r and a_θ from Eqs. (3) and (4), and then performing the averaging operation on the right-hand sides of the perturbation Eqs. (12) and (13) to retain only any remaining secular rate of change.

Equations in Terms of the True Anomaly θ

It is convenient to eliminate time as an independent variable in favor of θ through the use of Eq. (7). The form of the transformation is seen to be

$$\frac{\mathrm{d}}{\mathrm{d}t} = \frac{h}{r_G^2}\frac{\mathrm{d}}{\mathrm{d}\theta} + \mathcal{O}\left(\frac{\ell}{r_G}\right)^2 \tag{16}$$

and the terms of order $(\ell/r_G)^2$ can be neglected, since they would only introduce terms of higher order in Eqs. (9), (12), and (13). The new libration equation is then

$$\frac{\mathrm{d}}{\mathrm{d}\theta}\left[\frac{\ell^2}{r_G^2}\left(1 + \frac{\mathrm{d}\alpha}{\mathrm{d}\theta}\right)\right] = -\frac{3}{p}\frac{\ell^2}{r_G}\sin\alpha\cos\alpha \tag{17}$$

and the perturbation equations for e and ω become

$$\frac{\mathrm{d}e}{\mathrm{d}\theta} = \frac{r_G^2 p}{h^2}\left\{\sin\theta a_r + \left[\cos\theta + \frac{r_G}{p}(e + \cos\theta)\right]a_\theta\right\} \tag{18}$$

$$\frac{\mathrm{d}\omega}{\mathrm{d}\theta} = -\frac{r_G^2}{eh^2}[p\,\cos\theta a_r - (p + r_G)\,\sin\theta a_\theta] \tag{19}$$

In a similar spirit, the radius vector r_G can be related to θ within each orbit by the Keplerian law

$$r_G = p/(1 + e\,\cos\theta) \tag{20}$$

with e evolving secularly and with θ measured from the similarly evolving perigee.

III. Selection of Tether-Length Variation Laws

Since the objective is to obtain a continuing libration-orbit coupling, it seems clear that the length ℓ should be made to vary cyclically with θ; this will induce librations $\alpha(\theta)$ through the action of the Coriolis forces $2\dot{\theta}\dot{\ell}$, and these will have components in resonance with the orbital period even when this period is made to drift slowly. In the following sections we investigate the behavior of the system under such length modulations.

Length Variation to Maintain a Radially Pointing Tether

For a circular orbit, a constant-length tether, if otherwise unperturbed, will continuously point along the local vertical. For an elliptical orbit, the nonuniform orbital motion will excite librations with amplitude of the order of e.[5] On the other hand, if the tether length ℓ is made to vary in the same proportion as the radius vector r_G, i.e.,

$$\frac{\ell}{r_G} = \mathrm{const} \tag{21}$$

then it can be verified that $\alpha = 0$ is a solution of Eqs. (7) and (8) [or Eqs. (8) and (9)]. In this case, the orbital angular momentum $r_G^2\dot{\theta}$ remains strictly constant even within one orbit [see Eq. (7)], the azimuthal acceleration is zero [Eq. (4)], and

the radial perturbation a_r varies with r_G in the same way as the main gravitational acceleration [Eq. (3)]. Therefore, de/dt and $d\omega/dt$ [Eqs. (12) and (13)] vary as $\sin\theta$ and $\cos\theta$, respectively, and their averages over the orbit are zero. This length variation law occupies a neutral or central position among the possible laws, and we will refer to it as "the central law." If we want to obtain small libration angles about the radial direction, the natural approach is to investigate small deviations from the central length law.

First-Order Perturbations about the Central Law

Theory

Equation (17) can be rewritten as

$$\frac{d^2\alpha}{d\theta^2}+2\frac{d\,\ell n(\ell/r_G)}{d\theta}\frac{d\alpha}{d\theta}+3\frac{r_G}{p}\sin\alpha\cos\alpha=-2\frac{d\,\ell n(\ell/r_G)}{d\theta} \quad (22)$$

Since $\alpha=0$ is a solution when $\ell/r_G=\text{const}$, we expect to find $\alpha\ll 1$ for correspondingly small departures from the central law. Let us adopt a length variation law of the form

$$\frac{\ell}{r_G}=\left\langle\frac{\ell}{r_G}\right\rangle(1+\lambda_c\cos\theta+\lambda_s\sin\theta) \quad (23)$$

where $|\lambda_c|\ll 1$ and $|\lambda_s|\ll 1$. The maximum, minimum, and average tether length are related to λ_s, λ_c, and the eccentricity e through the expressions

$$\ell_{\substack{\max\\\min}}\simeq p\left\langle\frac{\ell}{r_G}\right\rangle\frac{1}{1\mp\sqrt{(e-\lambda_c)^2+\lambda_s^2}} \quad (24)$$

$$\bar{\ell}=p\left\langle\frac{\ell}{r_G}\right\rangle\left\{\left[1-\lambda_c\left(\frac{1-\sqrt{1-e^2}}{e}\right)\right]\Big/\sqrt{1-e^2}\right\} \quad (25)$$

In Eq. (25), the overbar is used to denote a one-orbit average. Equation (24) is valid only for $|\lambda_s|$, $|\lambda_c|\ll 1$.

Whenever λ_c and λ_s are small, $d\ell n(\ell/r_G)/d\theta\simeq-\lambda_c\sin\theta+\lambda_s\cos\theta$, and the second term in Eq. (22) can be neglected, since it contains the product of λ_s or λ_c times α, which is also small. Thus, the small-angle (but arbitrary eccentricity) libration equation becomes

$$\frac{d^2\alpha}{d\theta^2}+\frac{3\alpha}{1+e\cos\theta}=-2(-\lambda_c\sin\theta+\lambda_s\cos\theta) \quad (26)$$

It is clear from the form of this equation that the two types of perturbation, $\lambda_c\cos\theta$ and $\lambda_s\sin\theta$ can be dealt with separately and the results superimposed. The part $\lambda_c\cos\theta$ is seen to generate librations $\alpha(\theta)$ which are *odd* functions of θ, while $\lambda_s\sin\theta$ generates *even* $\alpha(\theta)$ librations.

For small α, $|\lambda_s|$, and $|\lambda_c|$, the perturbing accelerations, from Eqs. (3) and (4), are

$$a_r\simeq-\frac{3\mu}{r_G^2}\frac{m_{12}}{m}\left\langle\frac{\ell}{r_G}\right\rangle^2(1+2\lambda_c\cos\theta+2\lambda_s\sin\theta) \quad (27)$$

$$a_\theta\simeq\frac{3\mu}{r_G^2}\frac{m_{12}}{m}\left\langle\frac{\ell}{r_G}\right\rangle^2\alpha(\theta) \quad (28)$$

and substituting into the orbital perturbation equations [Eqs. (18) and (19)],

$$\frac{de}{d\theta}=3\frac{m_{12}}{m}\left\langle\frac{\ell}{r_G}\right\rangle^2\left\{-\sin\theta(1+2\lambda_c\cos\theta+2\lambda_s\sin\theta)+\left(\frac{e+\cos\theta}{1+e\cos\theta}+\cos\theta\right)\alpha(\theta)\right\} \quad (29)$$

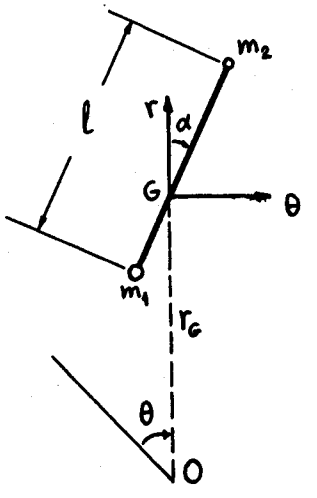

Fig. 1 Dumbbell geometry.

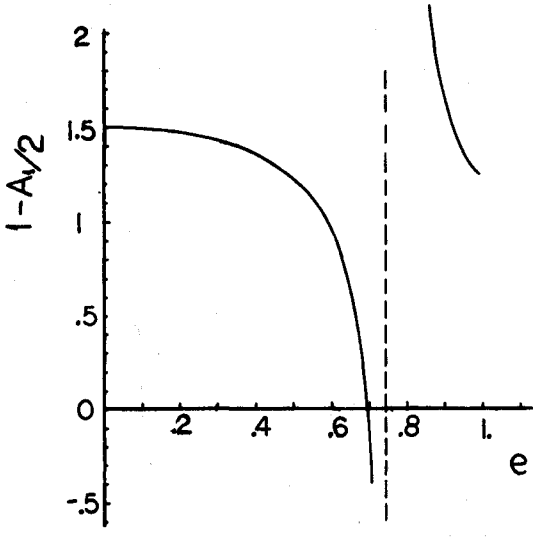

Fig. 2 Factor for Eqs. (37) and (38) vs orbital eccentricity.

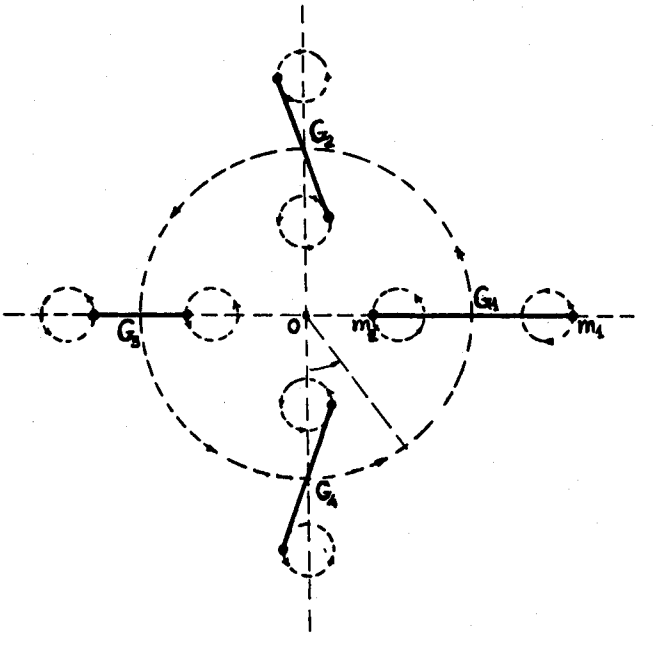

Fig. 3 Successive configurations of variable-length dumbbell through one orbit. G_4 will be raised and G_2 depressed.

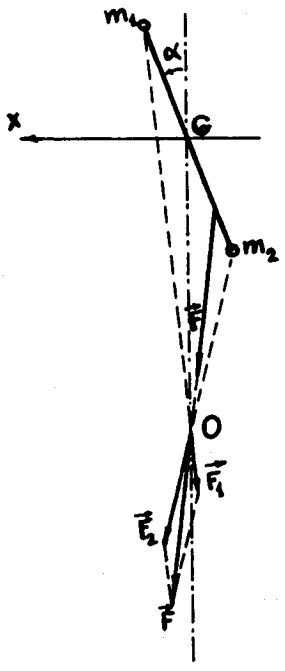

Fig. 4 Due to $|F_2| > |F_1|$ the resultant gravity force F has a component along X (plus a restoring torque).

$$\frac{d\omega}{d\theta} = -\frac{3}{e}\frac{m_{12}}{m}\left\langle\frac{\ell}{r_G}\right\rangle^2\left\{-\cos\theta(1+2\lambda_c\cos\theta + 2\lambda_s\sin\theta) - \left(1+\frac{1}{1+e\cos\theta}\right)\sin\theta\alpha(\theta)\right\} \tag{30}$$

These expressions would yield the detailed variations of e and ω within each orbit, once the solution $\alpha(\theta)$ of Eq. (26) is inserted. However, we are interested in the long-range variations only, and so we will perform a one-orbit average of Eqs. (29) and (30) before proceeding. Most of the terms have simple averages ($\langle\sin\theta\rangle = 0$, $\langle\sin\theta\cos\theta\rangle = 0$, $\langle\sin^2\theta\rangle = \langle\cos^2\theta\rangle = 1/2$, etc.). For the terms involving $1/(1+e\cos\theta)$, we use Eq. (26) and integration by parts to obtain

$$\begin{aligned}\left\langle\frac{e+\cos\theta}{1+e\cos\theta}\alpha\right\rangle &= \frac{1}{3}\left\langle(e+\cos\theta)\times\left(2\lambda_c\sin\theta - 2\lambda_s\cos\theta - \frac{d^2\alpha}{d\theta^2}\right)\right\rangle\\ &= -\frac{\lambda_s}{3} - \frac{1}{3}\left\langle(e+\cos\theta)\frac{d^2\alpha}{d\theta^2}\right\rangle\\ &= -\frac{\lambda_s}{3} - \frac{1}{3}\left\langle\sin\theta\frac{d\alpha}{d\theta}\right\rangle\\ &= -\frac{\lambda_s}{3} + \frac{1}{3}\langle\alpha\cos\theta\rangle\end{aligned}$$

and similarly,

$$\left\langle\frac{\sin\theta}{1+e\cos\theta}\alpha\right\rangle = \frac{\lambda_c}{3} + \frac{1}{3}\langle\alpha\sin\theta\rangle$$

With these results, we obtain

$$\frac{de}{d\theta} = 4\frac{m_{12}}{m}\left\langle\frac{\ell}{r_G}\right\rangle^2(-\lambda_s + \langle\alpha\cos\theta\rangle) \tag{31}$$

$$\frac{d\omega}{d\theta} = \frac{4}{e}\frac{m_{12}}{m}\left\langle\frac{\ell}{r_G}\right\rangle^2(\lambda_c + \langle\alpha\sin\theta\rangle) \tag{32}$$

We noted before that when $\lambda_s = 0$, the solutions to Eq. (26) are odd functions of θ, and hence $\langle\alpha\cos\theta\rangle = 0$. Therefore, for length variations of the type $1+\lambda_c\cos\theta$ ($\lambda_s = 0$), Eq. (31) shows that the eccentricity is not affected in the long run. A similar argument shows that length variations of the complementary type $1+\lambda_s\sin\theta$ will not affect the argument of perigee ω.

The form of Eqs. (31) and (32) indicate that rather than the complete solution of the libration equation [Eq. (26)], we need only find its first harmonics, which are uniquely related to $\langle\alpha\cos\theta\rangle$ and $\langle\alpha\sin\theta\rangle$. All the other harmonics of α contribute nothing to the long-term orbital evolution. Also, from the preceding discussion, it is clear that

$$-\frac{\langle\alpha\cos\theta\rangle}{\lambda_s} = \frac{\langle\alpha\sin\theta\rangle}{\lambda_c}$$

We therefore concentrate on the case $\lambda_c = 0$ and seek a solution for α in the form of a Fourier *cosine* series:

$$\alpha = \lambda_s(A_0 + A_1\cos\theta + A_2\cos2\theta + \cdots) \tag{33}$$

Substituting into Eq. (26) and collecting equal-order terms, we obtain the infinite system of equations

$$3A_0 - \frac{e}{2}A_1 = -e$$

$$2A_1 - 4\frac{e}{2}A_2 = -2$$

$$-\frac{e}{2}A_1 - A_2 - 9\frac{e}{2}A_3 = -e$$

and

$$-(n-1)^2\frac{e}{2}A_{n-1} - (n^2-3)A_n - (n+1)^2\frac{e}{2}A_{n+1} = 0 \qquad (n \geq 3) \tag{34}$$

The last line in Eq. (34) can be rewritten as

$$\frac{A_n}{A_{n-1}} = \left\{\left[-(n-1)^2\frac{e}{2}\right]\Big/\left[n^2 - 3 + (n+1)^2\frac{e}{2}\frac{A_n+1}{A_n}\right]\right\} \tag{35}$$

Thus, A_3/A_2 is related to A_4/A_3, which can in turn be related to A_5/A_4 and so on. This leads to a computationally convenient continued fraction expansion for A_3/A_2: we start from an approximate value for a ratio A_{n+1}/A_n ($n \gg 1$) and work backwards to A_3/A_2. For $n \to \infty$, it is easy to see from Eq. (35) that A_n/A_{n-1} tends to the limit $-e/(1+\sqrt{1-e^2})$, and this can be used as a starting value at some large but finite n. Once A_3/A_2 is found from this calculation, the values of A_0, A_1, and A_2 follow easily from the first three equations in Eqs. (34). Finally, then, we obtain

$$\langle\alpha\cos\theta\rangle = \frac{\lambda_s}{2}A_1 \tag{36}$$

and therefore also, if λ_c is not zero, $\langle\alpha\sin\theta\rangle = -(\lambda_c/2)A_1$. The perturbation Eqs. (31) and (32) reduce to

$$\frac{de}{d\theta} = -4\frac{m_{12}}{m}\left\langle\frac{\ell}{r_G}\right\rangle^2\lambda_s\left(1-\frac{A_1}{2}\right) \tag{37}$$

$$\frac{d\omega}{d\theta} = \frac{4}{e}\frac{m_{12}}{m}\left\langle\frac{\ell}{r_G}\right\rangle^2\lambda_c\left(1-\frac{A_1}{2}\right) \tag{38}$$

The factor $1 - A_1/2$ is plotted as a function of eccentricity in Fig. 2. For $e < 0.6$, an excellent approximation (error $< 0.4\%$) is given by the result of truncating the continued fraction expansion of Eq. (35) after the e^4 order:

$$1 - \frac{A_1}{2} \simeq \frac{3}{2} \frac{286 - 661e^2 + 150e^4}{286 - 518e^2 + 34e^4} \tag{39}$$

We note from Fig. 2 that the sign of $1 - A_1/2$ reverses at $e = 0.67$. In addition, we note a singularity at $e \simeq 0.747$. A more detailed Floquet analysis of Eq. (26) shows that at this value of e the homogeneous solutions $\alpha_1(\theta)$ and $\alpha_2(\theta)$ of Eq. (26) become periodic of period 2π. For $e < 0.747$, they are pseudoperiodic in that only their pytagoric sum $\sqrt{\alpha_1^2 + \alpha_2^2}$ is periodic while they are individually not, but they are bounded. The solutions α_1 and α_2 become again pseudoperiodic beyond $e = 0.747$, periodic again at $e = 0.994$, and unstable beyond that. The singularity at $e = 0.747$ has the nature of a resonance between the once-per-orbit driving terms and these periodic natural vibrations. For practical purposes, it appears from Fig. 2 that $e \simeq 0.6$ is the upper limit of usefulness of the particular "pumping" technique described here. Notice that $e = 0.6$ represents a ratio of apogee to perigee

$$\frac{r_a}{r_p} = \frac{1+e}{1-e} = 4$$

and this means the technique can be used to transfer between low Earth orbits ($r_p \simeq 300$ km) and orbits with an apogee as high as 20,000 km above the Earth's surface.

Example of Application

The apogee of an orbit with $e = 0.6$ and $R_{\text{perigee}} = 6650$ km ($h_{\text{perigee}} = 280$ km) is at $R_{\text{apogee}} = 26{,}660$ km. A circular orbit of this radius is of interest due to its period being exactly 12 h. We could envision a transfer to such an orbit in the following stages: 1) Hohmann transfer between LEO and some intermediate circular orbit, selected such that tether pumping from it will continuously deform this orbit into the 6650/26,600-km orbit. Since for the latter we can easily calculate $p = 2R_aR_p/(R_a + R_p) = 10{,}640$ km, this is also the radius of the desired circular orbit (p is uniquely related to angular momentum, and hence remains constant during pumping). 2)Tether pumping according to Eq. (23), with $\lambda_c = 0$, until the 6650/26,600 km orbit is reached. 3) Circularization with an apogee rocket burn into the 12 h orbit.

A simple calculation yields for maneuvers 1 and 3 a total required ΔV of 2397 m/s. For comparison, a normal Hohmann transfer from LEO to the 12 h orbit requires $\Delta V = 3471$ m/s. This savings of 1074 m/s can translate into very large fuel mass savings, which can be traded for the required tether and power system mass plus an increase in payload. Clearly the most favorable case for this application would be one where a large power supply is available onboard for other reasons, since, as will be seen, the pumping maneuver is quite power-intensive. As an example of the performance potential, consider a wide-body Centaur with a propellant load of 20,000 kg and a structural mass of 2950 kg. The direct Hohmann maneuver allows a payload of 15,000 kg to the 12 h orbit, while the maneuver with intermediate tether pumping would increase this to 24,700 kg. This increase of 9700 kg could amply accommodate the mass of the motorized reel and tether and even perhaps that of a 100 kWe nuclear-electric system (3000 kg projected for the SP-100 reactor), although, as mentioned, favorable missions may already include that as part of the payload.

As is common in other electric propulsion schemes, there is a tradeoff here between power level and mission duration. An approximate analysis[6] for our example gives a direct connection between the peak power $p_{\max}$, the length modulation factor λ_s, and the rate of eccentricity change (which is about constant for $e < 0.6$, see Fig. 2):

$$\frac{de}{d\theta} \simeq 2.75 \times 10^{-9} \lambda_s P_{\max} \tag{40}$$

If λ_s is taken to be 0.3 and $P_{\max}$ is 100 kW, Eq. (40) indicates that about 1000 orbits are required for an eccentricity change of 0.6. A simple integration of the varying orbital period then gives a pumping time of 151 days, which is commensurate with mission times for electric thrusters. Since the power requirements are cyclic, with positive and negative peaks several times higher than the mean power (see Sec. IV), a base-load 100-kWe generator may actually imply peak powers of 300–400 kW if flywheels or other storage devices are used, and this would result in direct reductions of the transit time. Alternatively, a smaller power supply could be used for the same transit time.

The combination of tether length and mass split between the two tether ends is governed by the available power (or the mission duration). For our example,[6]

$$P_{\max} = 5.73 \times 10^4 m_{12} \left\langle \frac{\ell}{r_G} \right\rangle^2 \tag{41}$$

and if we assume the mass can be divided evenly between the two ends, $m_1 = m_2 = \frac{1}{2}$ 33,150 kg (33,150 kg is the mass during pumping), and we take $P_{\max} = 100$ kW,

$$\left\langle \frac{\ell}{r_G} \right\rangle = 0.0145$$

The tether length is given by

$$\ell = r_G \left\langle \frac{\ell}{r_G} \right\rangle (1 + \lambda_s \sin\theta) = p \left\langle \frac{\ell}{r_G} \right\rangle \frac{1 + \lambda_s \sin\theta}{1 + e\cos\theta}$$

At the start of pumping, $e = 0$, $r_G = 10{,}640$ km and ℓ varies between 108 and 200 km in each orbit. At the end of pumping, $e = 0.6$, r_G goes from 6650 to 26,600 km, and ℓ varies in one orbit between 23.5 and 380 km. The tether tension is maximum near Earth, and so the tether thickness will be set by conditions pertaining to a length of the order of 100 km in LEO and is not expected to be excessive.

Near-Circular Orbits

By restricting our attention to cases with $e^2 \ll 1$, we can obtain more detailed solutions that give insight into the mechanics of the pumping action. These solutions are also directly useful for maneuvers between LEO orbits. For the present purposes, we will go back to the governing Eqs. (6), (7), and (8) instead of using the orbital element perturbation scheme. We will linearize the motion about a circular orbit at $r_G = R$, $\dot\theta = \Omega = \sqrt{\mu/R^3}$ where R is chosen such that

$$mR^2\Omega = L \tag{42}$$

i.e., the full angular momentum of the dumbbell (including that associated with its moment of inertia) is assigned to the reference point mass m orbiting at R. This could be physically realized by gradually reeling back to zero length so as to convert the angular momentum about the center of mass into additional orbital angular momentum without spinning the tether. It follows that R is somewhat above the acutal center of mass of the orbiting dumbbell. Putting

$$r_G = R + \rho; \qquad \dot\theta = \Omega + \omega \tag{43}$$

with $\rho \ll R$, $\omega \ll \Omega$, linearizing Eqs. (6–8) and eliminating ω, we obtain

$$\ddot\rho + \Omega^2\rho = -\frac{m_{12}}{m}\Omega^2\frac{\ell^2}{R}\left(2\dot\alpha + 5\Omega - \frac{9}{2}\Omega\sin^2\alpha\right) \tag{44}$$

and

$$\frac{\mathrm{d}}{\mathrm{d}t}[\ell^2(\dot{\alpha}+\Omega)] = -3\Omega^2\ell^2 \sin\alpha \cos\alpha \tag{45}$$

Once again we restrict our attention to small libration angles ($\alpha \ll 1$) and use the unperturbed true anomaly $\theta = \Omega t$ as the independent variable:

$$\frac{\mathrm{d}^2\rho}{\mathrm{d}\theta^2} + \rho = -\frac{m_{12}}{m}\frac{\ell^2}{R}\left(2\frac{\mathrm{d}\alpha}{\mathrm{d}\theta} + 5\right) \tag{46}$$

$$\frac{\mathrm{d}}{\mathrm{d}\theta}\left[\ell^2\left(1+\frac{\mathrm{d}\alpha}{\mathrm{d}\theta}\right)\right] = -3\ell^2\alpha \tag{47}$$

It can be directly verified that for a simple length variation law of the form

$$\ell = \langle\ell\rangle(1 + \lambda_s \sin\theta) \tag{48}$$

one particular solution to Eq. (47) is

$$\alpha = -\lambda_s \cos\theta \tag{49}$$

and it can be shown by a Floquet analysis that the two independent homogeneous solutions are quasiperiodic in θ, which guarantees nondivergence of the general solution. Assuming the initial conditions are chosen so as to produce the libration given by Eq. (49), then Eq. (46) is seen to contain a resonant forcing term:

$$\frac{\mathrm{d}^2\rho}{\mathrm{d}\theta^2} + \rho = -\frac{m_{12}}{m}\frac{\langle\ell\rangle^2}{R}(5 + 12\lambda_s \sin\theta) \tag{50}$$

where ℓ^2 has been expanded to linear order in λ_s. The general solution to Eq. (50) is

$$\rho = A \sin(\theta - \theta_0) - \frac{m_{12}}{m}\frac{\langle\ell\rangle^2}{R}(5 - 6\lambda_s\theta \cos\theta) \tag{51}$$

which contains a secularly growing term. For a large θ this term dominates, and ρ will go through maxima (apogee passages) at $\theta \simeq n(2\pi)$ (n = integer) and through minima (perigee passages) at $\theta \simeq \pi + n(2\pi)$. These points have radii

$$(r_G)_a \simeq R + 6\frac{m_{12}}{m}\frac{\langle\ell\rangle^2}{R}\lambda_s 2\pi n \tag{52}$$

$$(r_G)_p \simeq R - 6\frac{m_{12}}{m}\frac{\langle\ell\rangle^2}{R}\lambda_s(2n+1)\pi \tag{53}$$

giving, to the first order in $\langle\ell\rangle^2/R^2$, an eccentricity of

$$e = 12\pi\frac{m_{12}}{m}\left(\frac{\langle\ell\rangle}{R}\right)^2\lambda_s\left(n+\frac{1}{2}\right) \tag{54}$$

and hence, in the long run,

$$\frac{\mathrm{d}e}{\mathrm{d}\theta} = \frac{1}{2\pi}\frac{\mathrm{d}e}{\mathrm{d}n} = 6\frac{m_{12}}{m}\left(\frac{\langle\ell\rangle}{R}\right)^2\lambda_s \tag{55}$$

For the conventional orbital orientation (i.e., perigee at $\theta = 0$), a ($-$) sign ought to be appended to Eq. (55), since the increasing maximum radial perturbation occurs at the location of the current perigee. This expression coincides with the $e^2 \to 0$ limit of Eq. (37), since, according to Eq. (39), $1 - A_1/2 \to 3/2$ in that limit. Notice, incidentally, that the constant term $-5m_{12}/m\langle\ell\rangle^2/R$ in Eq. (51) represents the downward distance from the chosen reference R to the actual c.g.

The tension in the connecting tether can be calculated from the solution obtained for α. For a near-circular orbit, one obtains from Eq. (5) (to order ℓ^2/R^2)

$$T = m_{12}(3\Omega^2\cos^2\alpha + 2\Omega\dot{\alpha}^2)\ell - m_{12}\ddot{\ell} \tag{56}$$

and assuming small α and using Eqs. (48) and (49),

$$T = 3m_{12}\Omega^2\langle\ell\rangle(1 + 2\lambda_s \sin\theta) \tag{57}$$

Maximum tension occurs at maximum length ($\theta = 90$ deg) and vice versa. The minimum tension (and length) occurs halfway during the perigee-apogee transit if $\lambda_s < 0$, which corresponds to an increasing e. This minimum tension is reduced by a factor $1 - 2|\lambda_s|$ from its static gravity gradient value ($3m_{12}\Omega^2\langle\ell\rangle$), and hence a loss of tension would occur (to this approximation) for $|\lambda_s| > 1/2$ (length modulation between $1/2\langle\ell\rangle$ and $3/2\langle\ell\rangle$, libration amplitude 0.5 rad).

The instantaneous winding power is $-T\dot{\ell}$, or

$$P = 3m_{12}\Omega^3\langle\ell\rangle^2\lambda_s(1 + 2\lambda_s \sin\theta)\cos\theta \tag{58}$$

This power is maximum somewhere between $\theta = 135$ and 180 deg, and the maximum value of the trigonometric factor in Eq. (58) is shown in Table 1 as a function of λ_s. Notice that P, as given by Eq. (58), changes sign in going from θ to $\pi - \theta$. To this approximation, exactly equal amounts of power must be invested and withdrawn over one orbit, resulting in a zero *net* power input. This corresponds to the fact that for a fixed angular momentum, the orbital energy varies as $1 - e^2$, and since only first-order changes in eccentricity about $e = 0$ are considered, our present approximation is one of constant orbital energy.

A mechanistic interpretation of these results is now possible. From Eqs. (48) and (49), each of the end masses of the dumbbell can be seen to describe a circle once per orbit (of radii $\ell m_2/m|\lambda_s|$, $\ell m_1/m|\lambda_s|$ for masses m_1 and m_2, respectively) about their equilibrium positions. For $\lambda_s > 0$, this circle is described in the orbital direction. Maximum extension is reached at $\theta = 90$ deg, with the tether vertical (position G_1 in Fig. 3). As the tether contracts, Coriolis effects induce an advance (positive α) of the upper mass (position G_2), but the gravity gradient torque eventually restores verticality just as the minimum length is reached at $\theta = 270$ deg (position G_3). The process occurs in reverse between G_3 and G_1, through G_4 ($\theta = 0$). Notice that at G_2 the restoring gravity gradient torque is maximum in the direction tending to reduce the libration angular momentum. By the conservation of *total* angular momentum, this must also be the location of the maximum rate of *increase* of orbital angular momentum. How this is possible is indicated in Fig. 4, which follows a discussion by Murakami.[1] The resultant of the gravity forces $\boldsymbol{F}_1$ and $\boldsymbol{F}_2$ on the end masses has, as expected, a component producing the gravity-gradient torque about G. But, in addition, it also has a forward component when α is positive, and this is what produces the forward acceleration at location G_2 in Fig. 3 (and a corresponding deceleration at G_4). The accumulated effect of these forces is to raise G_4 and depress G_2, as indicated by Eqs. (52) and (53).

Second-Order Perturbations about a Constant Tether Length

We showed earlier that small libration angles could be maintained even in highly eccentric orbits if a basic length variation was adopted in which ℓ varied in direct proportion to the radius vector r_G. From an operational standpoint this implies a constant reel-unreel activity, even when no orbital changes are intended. On the other hand, we also saw that for near-circular orbits, cyclic length variations about a constant length are suffi-

Table 1 Maximum reeling power

λ_s	0	0.1	0.2	0.3	0.4	0.5
$p_{max}/(3m_{12}\Omega^3\langle\ell\rangle^2\lambda_s)$	1	1.019	1.068	1.136	1.212	1.299

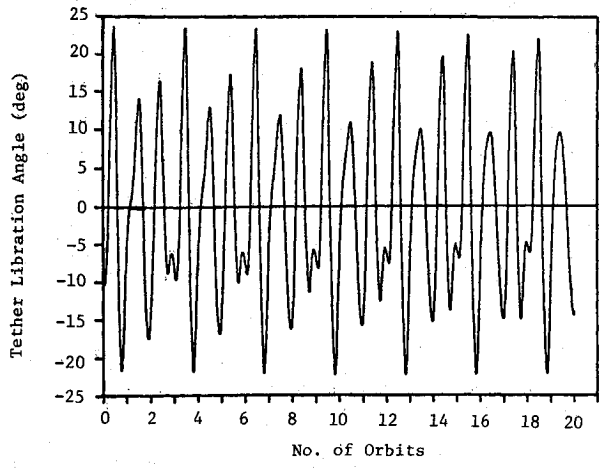

Fig. 5 Tether libration angle vs number of orbits over twenty orbits.

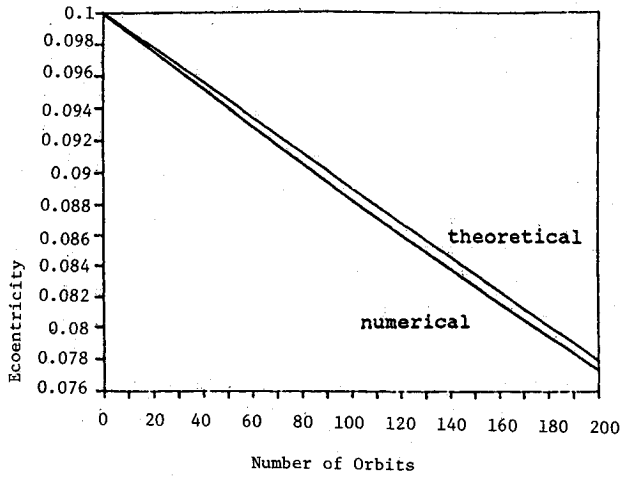

Fig. 6 Eccentricities vs number of orbits, analytical and numerical.

cient for orbital changes. Unfortunately, if this approach (cyclic length changes with constant mean length) is extended to orbits with nonnegligible eccentricity, the coupling between libration and orbital angular momentum changes will force librations even at constant length, and the smallness of α cannot be ensured even for small λ_s, λ_c. It is therefore of interest to examine the effect of increasing e on a pumping law of the simple form of Eq. (48), which is easier to implement than that of Eq. (23). The results of this analysis will only be summarized here; a detailed account can be found in Ref. 7.

The equations of motion and the variational Eqs. (17), (18), and (19), together with the length law of Eq. (48), can be expanded to second-order in e, α, λ_c and λ_s. Since α appears only in the form of $\sin\alpha$ or $\sin 2\alpha$, no quadratic terms in α occur, and the equations remain linear in the libration angle, which facilitates solution. In fact, the libration Eq. (17) can be shown to reduce to a Mathieu equation, whose solution to quadratic terms in e, λ_s and λ_c is quasiperiodic and contains terms at a variety of frequencies: 1) terms in $\sin(\sqrt{3}\theta)$, $\cos(\sqrt{3}\theta)$, and in $\sin\theta$, $\cos\theta$ (as in the limit $e^2 \to 0$), and 2) terms at combination frequencies; i.e., sines and cosines of 2θ, $(\sqrt{3} \pm 1)\theta$. The full expression is given in Ref. 6.

This general expression for the libration angle is then substituted into the orbital perturbation equations, which are then averaged on θ to eliminate terms with no secular growth. The results are

$$\frac{de}{d\theta} = -6\frac{m_{12}}{m}\left(\frac{\langle \ell \rangle}{a}\right)^2 \lambda_s \tag{59}$$

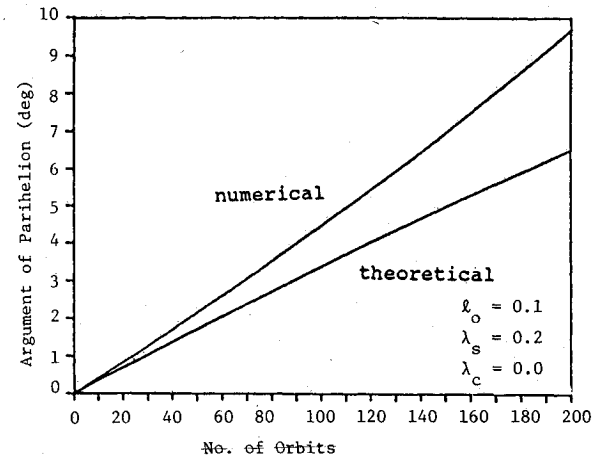

Fig. 7 Argument of perihelion vs number of orbits, analytical vs numerical.

$$\frac{d\omega}{d\theta} = 6\frac{m_{12}}{m}\left(\frac{\langle \ell \rangle}{a}\right)^2 \left(1 + \frac{\lambda_c}{e}\right) \tag{60}$$

and from the constancy of $p = a(1 - e^2)$,

$$\frac{da}{d\theta} = -12\frac{m_{12}}{m}\left(\frac{\langle \ell \rangle}{a}\right)^2 e\lambda_s \tag{61}$$

Notice the absence of quadratic terms in λ_s, λ_c in these equations, which are, however, accurate to the second order in these quantities. Equation (59) reduces to Eq. (55) for a near-circular orbit. Since a now varies with e [$a = p/(1 - e^2)$], a simple integration yields

$$e = \frac{1}{\sqrt{2}} \tanh\left[\tanh^{-1}(\sqrt{2}e_0) - \frac{N}{N^*}\right] \tag{62}$$

where N is the number of orbits described ($\theta/2\pi$) and N^* is given by

$$\frac{1}{N^*} = 12\sqrt{2\pi}\frac{m_{12}}{m}\left(\frac{\langle \ell \rangle}{p}\right)^2 \lambda_s \tag{63}$$

Equation (60) shows that the orbit of a dumbbell will rotate even in the absence of length variations ($\lambda_c = 0$). This effect arises from the coupling between the orbital angular momentum and the libration oscillations induced by the eccentricity itself; its contribution to the perigee rotation is discussed by Beletskii (Ref. 3, Ch. 5) for the case of a planet-like object. For a 100-km tether in LEO and for $m_1 = m_2$, this rotation would amount to about 0.13 deg per orbit (independent of eccentricity, to order e^2, and in the forward direction). For a tether length of about 150 km, this would cancel the rotation rate of a polar orbit due to Earth's oblateness: a passive tether of this length could, for instance, maintain its apogee over the North Pole permanently, a feature of potential interest for observation satellites. The apogee could easily be rotated to other locations by appropriate pumping, since length variations of the type $\lambda_c \cos\theta$, i.e., in phase with the radius vector variations, will also contribute to perigee rotation, according to Eq. (60). In fact, for $\lambda_c = -e$, this effect will exactly cancel that of the orbit-induced librations, and this is precisely the case in the "central law" type of length variation, i.e., when ℓ varies in proportion to r_G. We conclude this section by noting that the ratio of Eqs. (59) and (60) can be easily integrated to give

$$\omega - \omega_0 = -\frac{e - e_0}{\lambda_s} - \frac{\lambda_c}{\lambda_s} \ell n \frac{e}{e_0} \tag{64}$$

which, together with Eq. (62), serves to calculate $\omega(N)$.

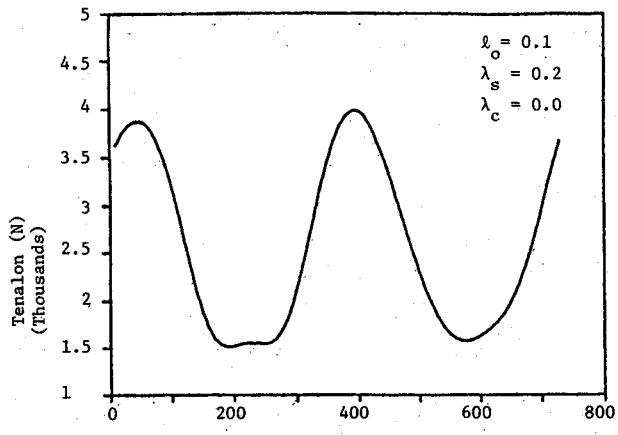

Fig. 8 Tension vs true anomaly over two orbits.

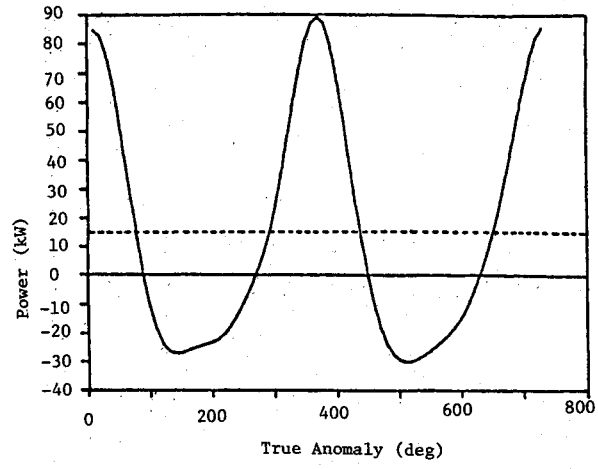

Fig. 9 Power vs true anomaly over two orbits.

IV. Computer Simulations

To verify the previous analysis, the theoretical variations in the orbital parameters derived in the previous subsection were compared to purely numerical results obtained by integrating the equations of motion of the center of mass of the tether system [Eqs. (6), (7), and (8)]. Several simulations were run for various initial conditions including positive, negative, and zero values for λ_s and λ_c. In the worst cases, both the theoretical eccentricity and semimajor axis were well within 1% of their numerical values. The theoretical argument of perihelion, however, only came within 6% of the numerical value in the best case. For better accuracy, one would have to consider third and higher order terms not kept in the theoretical analysis, probably because the small parameter λ_c is divided by the also small e in Eq. (60).

As an example, consider decreasing the eccentricity of an orbiting system using a sine variation of the tether length ($\lambda_s = 0.2$, $\lambda_c = 0.0$, a maximum tether length of 90 deg past perigee and a minimum tether length of 90 deg before perigee). Assume a lower mass of 100,000 kg connected to an upper mass of 10,000 kg via a variable-length tether with a mean length of 100 km. Also assume that the reeling operation begins when the system is at perigee or radius 6770 km.

Figure 5 shows the libration angle as a function of the number of orbits completed. The libration angle is a nonperiodic, bounded function with a maximum value of 24 deg. The numerical eccentricity and argument of perihelion are plotted vs the number of orbits completed in Figs. 6 and 7. The eccentricity can be reduced from 0.1 to 0.0773 in 200 orbits or approximately 15 days, while the argument of perihelion increases from 0 to 9.7 deg.

Now, consider the tether velocity, tension, and power requirements for the reeling operation. The derivative of the tether-length Eq. (48) yields a near-sinusoidal variation in the tether velocity with a maximum value of 24 m/s. The instantaneous tether tension described by Eq. (5) is plotted vs the number of orbits completed in Fig. 8. The average and minimum tensions observed are approximately 2750 and 1500 N, respectively, far from the danger of zero-tension tether.

The instantaneous power required for the reeling operation (which is the product of the tether velocity and tension) is shown in Fig. 9. A positive power indicates energy absorption by the reel mechanism (tether extension under tension), and this is seen to predominate in this example over the creation of mechanical work (rewinding under tension). This is in agreement with the fact that the semimajor axis a is decreasing as e decreases. The mean rate of energy absorption is seen to be 15 kW, while the peak absorption is 90 kW and the peak motoring power is 30 kW.

Since the length law considered did not include a variation proportional to the radius vector, increasing the eccentricity for a given length modulation depth leads to a higher and higher libration amplitude and eventually to the tether system spinning (α unbounded). The same result occurs when the length modulation is increased at constant eccentricity. Figure 10 shows the boundary of "stability" (α bounded vs unbounded) in an $e - \lambda_s$ map for $\lambda_c = 0$, $\langle \ell \rangle = 100$ km in LEO. Eccentricities or modulation depths greater than about 0.3 can be seen to lead to instability for this mode of pumping.

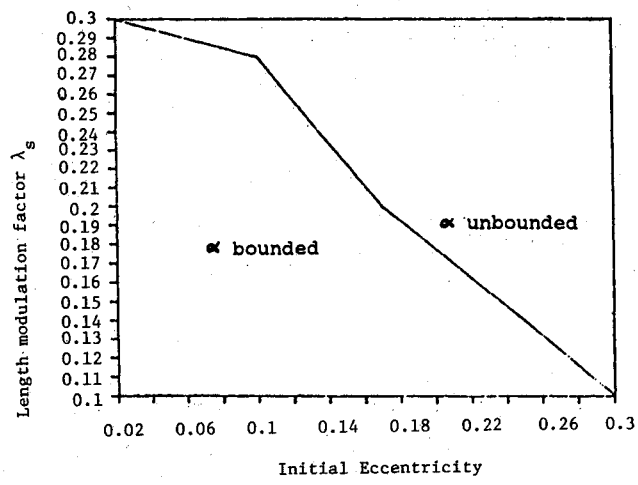

Fig. 10 Stability map for pumping about a constant length.

V. Examples of Application to Space Station Maneuvers

Some of the most promising near-term applications of the orbital pumping technique occur in conjunction with other tether applications, where the tether system is available to begin with. As examples, we show here how pumping could be combined with two proposed applications[8] of tethers to a Space Station: releasing GEO-bound OTV vehicles, and releasing a returning Space Shuttle.

Preconditioning of Station Orbit Prior to OTV Release

References 8 and 9 describe and analyze the use of an upward-pointing tether attached to an orbiting Space Station as a momentum-exchange device, by means of which an OTV can be launched with less expenditure of rocket fuel. The Station itself, initially in a circular orbit, loses momentum upon the tethered release of the OTV and enters and elliptical orbit with apogee at the release point and with a lower perigee, the altitude of which depends on the tether length selected. Reference 8 recommends making up the lost orbital energy by means of downwards Shuttle releases (see the following subsection).

Even if this is done, there will be periods of several weeks during which the station will be in an elliptical orbit, complicating the Shuttle rendezvous and perhaps other operations.

Given the presence of a tether facility on the Station, it would be relatively simple to use it for tether pumping, either to restore the orbit to circularity after release, or, probably better because of the extra end mass of the OTV, to precondition the orbit prior to release. The following example is taken from Ref. 6, where further details are given. Consider a 100,000-kg Station initially in a 450/450-km altitude. A 20,000-kg OTV is deployed to the end of a 100-km tether, and then, for a period of 2.1 days (33 orbits), the tether is pumped according to Eq. (48) with $\lambda_s = 0.2$. At this point, the center of mass of the Station-OTV has an eccentricity of 0.0073, and the semimajor axis is virtually identical to the initial radius. If the OTV is now released at a perigee passage, it receives an equivalent ΔV of 169 m/s, which, for example, translates into a 15% payload increase to geosynchronous orbit for an IUS vehicle.[9] Simultaneously, the Station circularizes its orbit at the altitude of the release, i.e., 67 km lower than the initial orbit.

The net effect of the maneuver is therefore to transfer to the OTV the difference between the angular momenta in the initial and final *circular* station orbits. For comparison, if no pumping is used before release with the same tether, the ΔV gain for the OTV is just about the same (168 m/s), but 1) the Station is left in an eccentric orbit, and 2) the perigee of this orbit is 117 km below the original height (instead of 67 km).

The tension during the pumping phase in this example varies between 8765 and 3757 N, and the power oscillates between approximately ± 150 kW, with a very small *net* power. The peak power can be reduced, say, by 50%, by pumping with half the amplitude ($\lambda_s = 0.1$) with the same tethered length. This preserves the same ΔV for the OTV, but makes the pumping phase twice as long.

Circularizing the Station's Orbit after Downward Shuttle Release

This is in essence the inverse of the maneuver just described. Reference 8 has identified tethered deorbiting of the Shuttle as one of the most attractive uses of a Station-attached tether, with more than sufficient reboosting capabilities to compensate for orbital station drag. Once again, circularity is upset upon each Shuttle release, and tether pumping can be used to correct this problem.

In this instance, using the Shuttle mass as the end mass during pumping is probably precluded by operational needs. Instead, a second, upwards-pointing tether (likely to be simultaneously present for OTV launches) can be used for this purpose, with an end mass, here taken to be 10,000 kg, that can be a remote docking-releasing teleoperator or some other tethered facility. The best time to execute the pumping is *after* the Shuttle release, when the Station-end mass is least; compared to prepumping (as in the previous subsection), this approach allows a higher initial Station *apogee* immediately after release, but this should pose no problems.

As an example, if the Station mass is 100,000 kg, the Shuttle mass 80,000 kg, the "dummy mass" on the upper tether is 10,000 kg, and the station starts deploying the Shuttle downwards from a 408/408-km orbit, a tether length of 56.2 km will ensure that, upon release, the Shuttle will have a perigee altitude of 180 km, the minimum acceptable for safety and from which reentry can be easily started with substantial savings in OMS fuel. The Station will itself be boosted to a 434/574-km orbit with an eccentricity of 0.0103. If the 10,000-kg upper mass is now deployed with a 100-km upper tether and pumping is executed with $\lambda_s = 0.2$, $\lambda_c = 0$, this eccentricity can be cancelled in 5.3 days (80 orbits), leaving the Station in a 504/504-km orbit. The tension varies between 26 and 468 N and the power oscillates between ± 79 kW during this pumping phase. As in the previous example, mission duration can be traded for peak power by controlling the length modulation depth.

VI. Discussion

The approach taken in this paper has been to study the effects of a series of prescribed tether-length variation laws, in particular those which are small perturbations about either a constant tether length or a length proportional to the radius vector. To varying degrees, both types of variation were shown to be limited by the onset of unbounded librations as the orbital eccentricity increases. An alternative approach would be to prescribe a desired libration angle $\alpha(\theta)$ and then use our Eq. (22) to extract the required length $\ell(\theta)$. This leads to tether-length laws applicable at any eccentricity, at the cost of some complexity in the length control. Closed-loop techniques would presumably be used to maintain the desired angle variations. This approach, suggested by one of the reviewers, will be the object of a forthcoming publication.

VII. Conclusions

The main conclusions of our study are as follows: 1) Tether-length variations ("pumping") synchronized to the orbit can be used to modify the eccentricity, energy, or argument of perigee of a satellite orbiting a spherical planet. The orbit parameter is a constant of the motion, however. 2) Length variations that maintain small libration amplitudes must be close to proportional to the radius vector to the satellite's center of mass. 3) For near-circular orbits, the orbital energy is only weakly affected by pumping (despite changes in eccentricity), but substantial changes (positive or negative) of energy can be effected for eccentric orbits by pumping in phase quadrature to the radius vector. 4) The line of apsides rotates forward even with a constant, but nonzero, tether length. Additional (forward or backward) rotation can be induced by pumping in phase with the radius vector. The rotation rate can in many cases exceed that due to Earth oblateness. 5) Most applications are power-limited in a manner similar to electric propulsion. Where a tether and power are available for other purposes (such as in a future space station), important applications of pumping are possible as supplements to other tether uses.

References

[1]Murakami, C., "On Orbit Control Using Gravity Gradient Effects," Paper IAF-80-E-218, presented at the XXX Congress of the IAF, Tokyo, 1980.

[2]Beletskii, V. V. and Givertz, M. E., "The Motion of an Oscillating Dumbbell Subject to a Gravitational Field," *Space Research*, Brief Report, Ref. 2, 1968.

[3]Beletskii, V. V., "Science," *Motion of an Artificial Satellite About its Center of Mass*, Moscow, 1965, translated as NASA TT F-429, 1966.

[4]Battin, R. H., *Astronautical Guidance*, McGraw-Hill, New York, 1964.

[5]Kaplan, M. H., *Modern Spacecraft Dynamics and Control*, J. Wiley & Sons, New York, 1976.

[6]Martinez-Sanchez, M., Gavit, S. A., and Stuart, D. A., "A Study of Transportation Applications of Space Tethers," Final Report to Martin Marietta Aerospace, Contract RH4-394007, Feb. 1985.

[7]Gavit, S. A., "Varying Tether Length for Modifying Orbital Eccentricities," M.S. Thesis, MIT, Dept. of Aero/Astronautics, Jan. 1985.

[8]"Selected Tether Applications in Space," Phase II Final Report, submitted by Martin Marietta to NASA, Contract NAS8-35499, Feb. 1985.

[9]Martinez-Sanchez, M. and Gavit, S. A., "Transportation Application of Space Tethers," AIAA/NASA Space Systems Technology Conference, Costa Mesa, CA, June 1984.